


Spin-Selective Equilibration among Integer Quantum Hall Edge Channels

Giorgio Nicolí¹,* Christoph Adam¹, Marc P. Rössli¹, Peter Märki¹, Jan Scharnetzky,
Christian Reichl, Werner Wegscheider¹, Thomas M. Ihn¹, and Klaus Ensslin¹
Solid State Physics Laboratory, ETH Zürich, 8093 Zürich, Switzerland

 (Received 3 August 2021; revised 3 January 2022; accepted 10 January 2022; published 3 February 2022)

The equilibration between quantum Hall edge modes is known to depend on the disorder potential and the steepness of the edge. Modern samples with higher mobilities and setups with lower electron temperatures call for a further exploration of the topic. We develop a framework to systematically measure and analyze the equilibration of many (up to 8) integer edge modes. Our results show that spin-selective coupling dominates even for non-neighboring channels with parallel spin. Changes in magnetic field and bulk density let us control the equilibration until it is almost completely suppressed and dominated only by individual microscopic scatterers. This method could serve as a guideline to investigate and design improved devices, and to study fractional and other exotic states.

DOI: [10.1103/PhysRevLett.128.056802](https://doi.org/10.1103/PhysRevLett.128.056802)

Quantum Hall devices remain paradigmatic for research on topological systems [1]. The Hall regime is accessed with a quantizing magnetic field perpendicular to a two-dimensional electron gas (2DEG) [2,3]. Dissipationless nonequilibrium currents flow in one-dimensional chiral channels along the edge of the system in response to an external voltage [4–7], experiencing inter-edge-state scattering in the presence of a background disorder potential [8–14]. Equilibration phenomena among nonequilibrium edge currents are not yet fully understood despite the rich history of past experiments on semiconducting devices.

Haug and co-workers found length-dependent equilibration in spin-degenerate quantum Hall systems with top gates acting as partially transmitting barriers [6,9,15], but did not report about spin-related effects. Later, Müller found that in the presence of a background disorder potential, spin-orbit interactions mediate the equilibration between spin-polarized edge modes by allowing charge carriers to flip their spin [11,16]. The continuous advancements in material technologies thus motivated a revival of equilibration experiments [17–20].

Local probe experiments by Weis *et al.* already showed the complexity of the microscopic reconstruction of the edge potential [21–24]. Further details on the edge could be revealed assuming that the presence of an incompressible region of a specific filling factor between two channels implies weak equilibration.

Quantum Hall edge state equilibration experiments gradually expanded to the fractional regime too, often finding nontrivial edge reconstructions and current distributions [25–27]. Graphene is another mature platform for quantum Hall experiments unraveling the role of valley and spin degrees of freedom in equilibration phenomena [28–31].

In this Letter, we address the question of inter-edge-mode scattering in state-of-the-art devices using electronic transport experiments. The design that we use is inspired by historically well-known experiments, where edge channels can be reflected and transmitted with barrier gates to obtain well-controlled out-of-equilibrium population of edge modes [15,16,32–34]. We study how the excitation of selected integer edge modes is redistributed as they co-propagate and extract the strength of pairwise coupling among many channels (up to 8). We find that the spin of the modes determines the equilibration at low enough fields, spin selectively coupling even distant channels in contrast with many findings from the past [6,8,11,12]. For larger fields the equilibration is almost completely suppressed and mesoscopic impurities dominate the weak equilibration between spin-split channels.

Our device is an MBE-grown [Al]GaAs heterostructure equipped with a patterned back gate located roughly $1\ \mu\text{m}$ below the plane of the 2DEG [35,36]. We lithographically defined top gates as indicated in Fig. 1(a). While the back gate tunes the whole device, we locally control the electron density with the injector and detector gates, creating tunable barriers in front of the injector and detector contacts. An additional gate located between the barriers on the side of the device pushes the 2DEG away from the physical edge of the mesa and creates a smooth electrostatic edge. A dilution refrigerator lowers the device temperature to $\lesssim 30\ \text{mK}$. From previous characterization, we expect the 2DEG to thermalize with the lattice in our setup [37,38].

At integer filling factors of the 2DEG, an external magnetic field B induces edge conduction with the chirality indicated in Fig. 1(a). Following the Landauer-Büttiker formalism [40,41], the number of channels transmitted by each barrier depends on the local filling factors

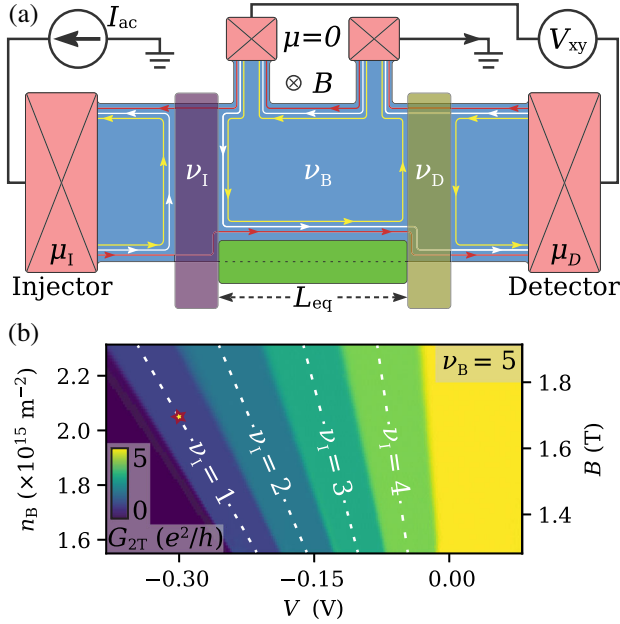


FIG. 1. (a) Schematic device structure and measurement setup, not to scale. A current $I_{ac} = 500$ pA flows through the device between injector and ground contacts, at potentials μ_I and $\mu = 0$, respectively. Two top gates act as barriers downstream of the injector (violet gate) and upstream of the detector (yellow gate) contacts. They are controlled via two dc voltage sources V_I and V_D (not shown). A side gate (green) laterally depletes the 2DEG along a length $L_{eq} = 35$ μm . (b) Two-terminal conductance measured through the device as a function of the left barrier gate voltage V_I . The right barrier gate is grounded [39]. The magnetic field B and bulk density n_B , controlled with the back gate, are stepped together to ensure constant bulk filling factor $\nu_B = 5$. Diagonal dashed lines indicate regions of constant conductance, corresponding to a quantized local filling factor ν_l below the injector gate.

$$\nu_{I,D} = \frac{hn_{I,D}}{eB} \leq \nu_B, \quad (1)$$

where ν_I and ν_D are the filling factors of the 2DEG under the injector and detector gates, respectively, when we fix the local densities to n_I and n_D . We tune the system such that ν_I, ν_D and the bulk filling factor ν_B have integer values to perform the experiments in a controlled way and suppress bulk equilibration [19]. We can route channels carrying different electrochemical potentials to flow along the co-propagation path [L_{eq} in Fig. 1(a)]. Measuring the longitudinal resistance across this path [6,11] or the potential of the detector with respect to ground (our case), will yield information about the strength of the equilibration processes among the channels.

We measure the two-terminal conductance G_{2T} as a function of the barrier voltage V_I while an ac current I_{ac} flows from the injector to ground and the other barrier is fully transparent. Figure 1(b) shows the result measured at $\nu_B = 5$. Plateaus of constant conductance matching integer

multiples of e^2/h are found as the barrier gate voltage decreases, (white dashed lines). Each diagonal feature corresponds to a fixed number of channels transmitted through the barrier region. We repeat the same experiment with the detector gate and for different bulk filling factors to observe the transmission characteristics of both barriers (not shown).

After flowing through the injector barrier, the transmitted channels will have a different electrochemical potential μ_i compared to the reflected modes on the other side of the barrier, coming from the grounded contact [cf. red versus yellow and white lines in Fig. 1(a)]. However, measuring the transverse voltage V_{xy} between the detector and ground will reveal no details about intermode coupling along the path if all channels equilibrate in the detector ($\nu_D = \nu_B$) [42]. The contact settles at the electrochemical potential

$$\mu_D = \frac{1}{\nu_D} \sum_{i=1}^{\nu_D} \mu_i, \quad (2)$$

where μ_i is the potential of an individual channel i when entering the detector. In the integer regime, all channels have transmission of one and contribute equally to the potential of the contact. When the detector barrier allows only selected modes to be transmitted ($\nu_D < \nu_B$), measurements of the transverse resistance will yield

$$R_{xy}^{(\nu_D)} = \frac{V_{xy}}{I_{ac}} = \frac{h}{e^2} \frac{\mu_D}{\nu_I \mu_I} = \frac{h}{e^2} \frac{1}{\nu_I \nu_D} \sum_{i=1}^{\nu_D} \frac{\mu_i}{\mu_I}. \quad (3)$$

The total equilibration between the channels does not depend on the specific tuning of the barriers, but rather on the edge potential along the propagation path, on the mesoscopic disorder background and on the length of co-propagation. Equilibration among channels under the detector gate does not affect the measurements [42]. If the external current is completely injected in the outermost channel ($\nu_I = 1$), an out-of-equilibrium population of spin-polarized electrons is built up. This channel can equilibrate either with other channels of the same spin polarization, or with channels of the opposite spin, if spin flips are involved.

We devised a measurement protocol to extract the electrochemical potential of the channels at the detector. We measure $R_{xy}^{\nu_D}$ for different values of ν_D while the injector barrier is tuned to $\nu_I = 1$. A system of equations of the form of Eq. (3) with values $1 \leq \nu_D \leq \nu_B$ describes the measurements [see Fig. 2(a)]. We can solve the system to find the normalized electrochemical potentials of the channels $\tilde{\mu}_i = \mu_i/\mu_I$, with the initial conditions $\tilde{\mu}_1^0 = 1$, and $\tilde{\mu}_j^0 = 0$ for $j \neq 1$.

Figures 2(b)–2(f) show the results of the analysis for different ν_B and in a range of magnetic fields and bulk densities. In Fig. 2(b)–2(d), we observe that electrons preferentially equilibrate with states of the same spin,

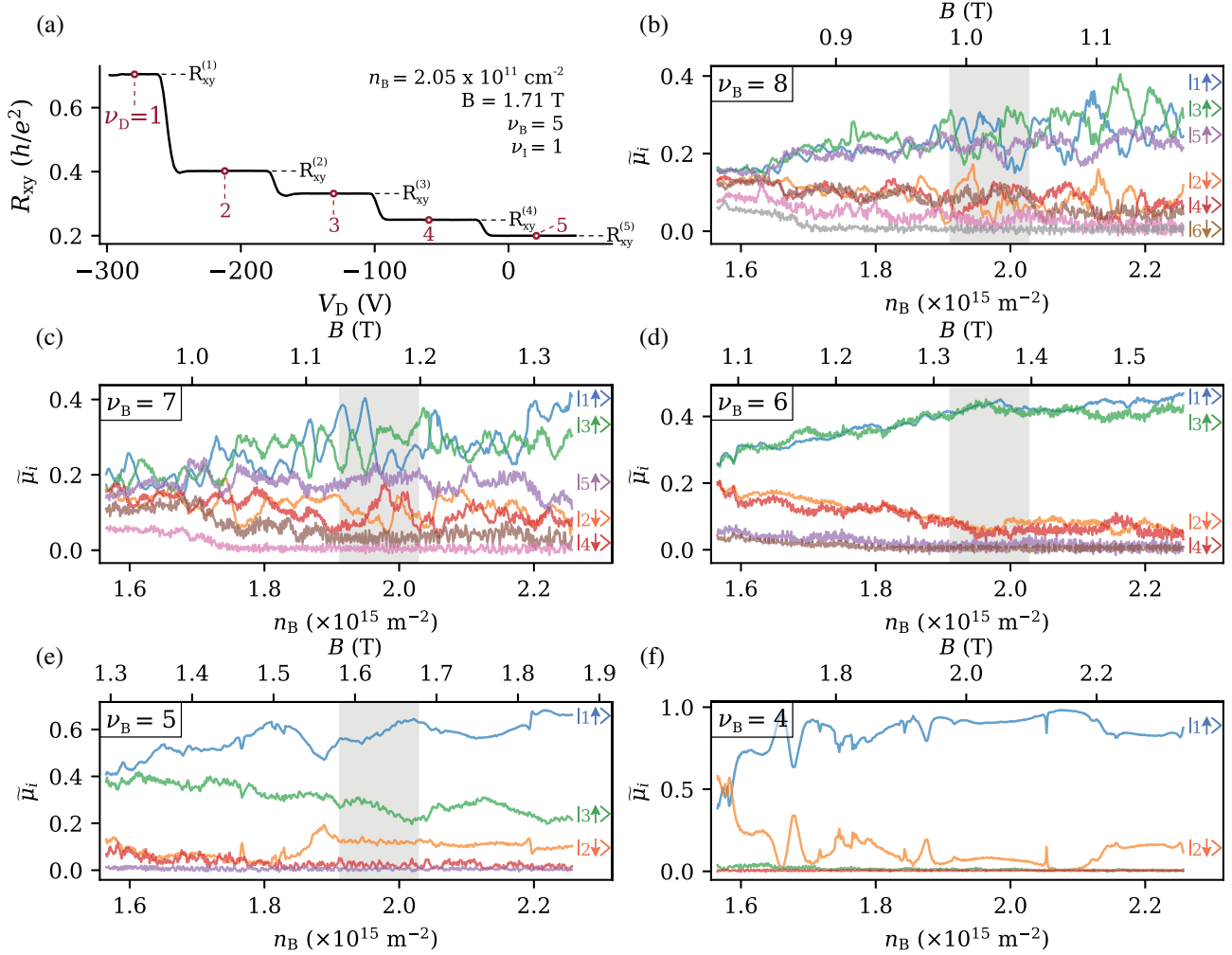


FIG. 2. (a) Equilibration measurement performed at the star-shaped symbol in Fig 1(b). The red circles indicate the data points required to calculate a set of $\tilde{\mu}_i$ following Eq. (3). (b)–(f) Electrochemical potential $\tilde{\mu}_i$ of the modes for integer bulk filling factors $\nu_B = 8$ –4 after the equilibration path. Matching labels indicate the spin and index of the channels. The back gate voltage V_{BG} (controlling n_B) and the magnetic field B are simultaneously stepped to fix ν_B during each experiment, similar to Fig. 1(b). The shaded regions in (a)–(d) indicate the range where coupling parameters have been extracted [see text and Fig. 3(c)–3(f)]. The data in (a) and (e) cannot be directly compared since they were collected at different times.

leaving channel 1 to occupy states in modes 3 and 5. Channels labeled with even numbers were mostly decoupled from the only initially excited channel and their potential is closer to the bottom of our energy scale.

In particular, when $\nu_B = 8$ or 6, two bundles of channels with opposite spin are resolved and well separated in energy. Even though the clear separation between the two bundles is not visible for the case of $\nu_B = 7$, also here the system favors spin-selective equilibration. The presence of reproducible fluctuations is likely due to impurities occurring on mesoscopic length scales, modulating the coupling between the modes [43].

If the three spin-up channels in Fig. 2(b) completely equilibrate while the others do not participate, we expect to find $\tilde{\mu}_{1,3,5} = 1/3 \simeq 0.33$, a case nearly reached at the

highest densities. Conversely, if all channels equilibrate, then $\tilde{\mu}_i = 1/8 = 0.125$ for all of them, which is nearly the case at the lowest densities.

As the number of channels in the bulk decreases with increasing external magnetic field, so does the coupling between them. Figure 2(e) ($\nu_B = 5$) shows that electrons in channels 1 and 3 are not fully equilibrating along L_{eq} , contrary to the cases with $\nu_B > 5$. We observe that the coupling becomes weaker for larger B , but spin-selective equilibration still remains the favored process. In Fig. 2(f) ($\nu_B = 4$) the coupling weakens to the point where $\tilde{\mu}_1 \approx \tilde{\mu}_1^0 = 1$ for the whole range. Few mesoscopic features increase the coupling between the two modes in the lowest Landau level, which requires some spin-flip mechanism. Spin-selective equilibration is not observed in this case.

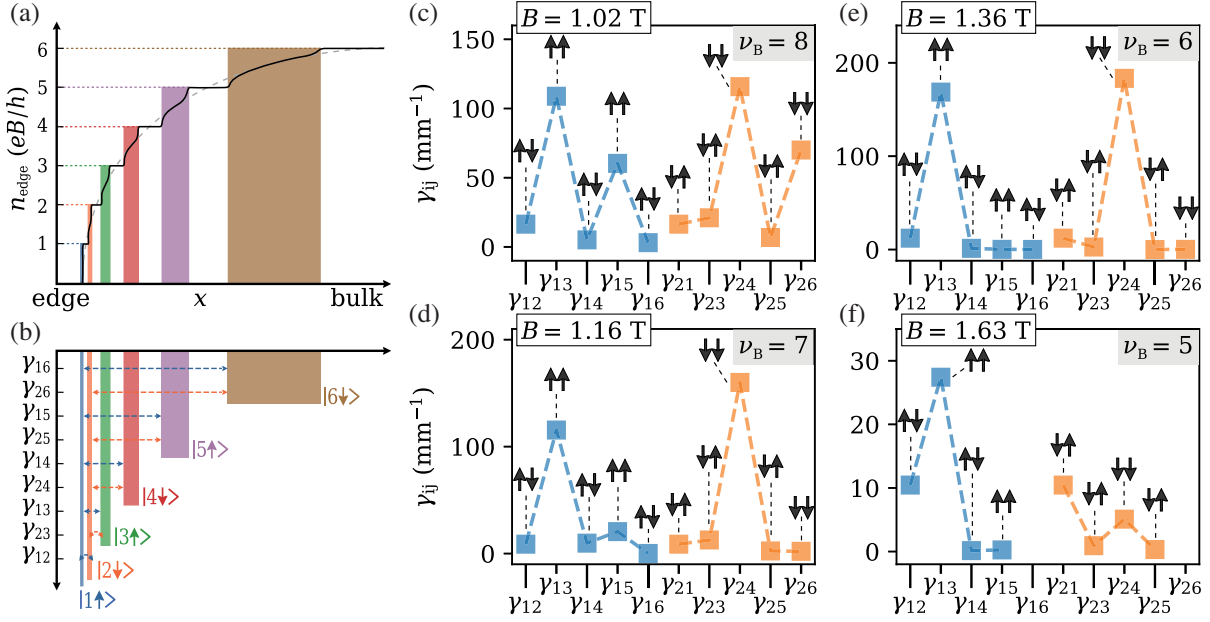


FIG. 3. (a) Density profile at the edge of the 2DEG. The unperturbed curve (gray dashed line) was calculated following Ref. [45]. The reconstructed density profile is sketched on top with colored shaded regions indicating the compressible stripes. (b) Pictorial representation of channels flowing along one edge of the device. A vertical axis labels the coupling terms represented as horizontal dashed arrows. Even though in our model we consider pairwise coupling terms γ_{ij} between all channels, the sketch shows only terms involving the two outermost channels (1 in blue and 2 in orange). (c)–(f) Coupling parameters for different bulk filling factors. The arrows indicate the spin alignment of the channels coupled by each term. The values reported here are averaged in the grey shaded areas in Fig. 2(b)–2(e). The central magnetic field for each shaded area is reported in the figure. The corresponding density range $n_B = 1.91\text{--}2.03 \times 10^{15} \text{ cm}^{-2}$ is the same for each plot.

Performing the same experiments over a distance $L'_{\text{eq}} = 535 \mu\text{m}$ reveals full equilibration irrespective of the spin alignment, although the innermost channel remains decoupled [42].

The density profile at the edge, sketched in the spirit of Ref. [44] in Fig. 3(a), guides us in understanding the results of Fig. 2. The edge channels represent discrete conducting regions located where the density has a nonzero gradient. Incompressible stripes with a fixed filling factor separate compressible regions that form at the edge as a result of screening and interactions in the presence of an external B field [44–47]. Decreasing ν_B at constant density, by increasing B , means that a smaller number of channels spans the density profile, pushing the innermost channels further into the bulk [21,26,48]. Increasing B and n_B while keeping ν_B constant instead results in wider incompressible stripes and a larger separation between the channels. The magnetic length ℓ_B , and, consequently, the spatial extent of the wave function of the edge modes, decreases for stronger fields. Since charge transfer between channels requires wave function overlap, a larger distance and stronger confinement can quickly suppress the tunneling probability amplitude.

Electrons can, in principle, tunnel from one channel to any other, conserving or flipping their spin. The energy transfer between modes can be approximated with a system of rate equations of the form [42]

$$\frac{d\mu_i}{dx} = -\frac{1}{2} \sum_{j \neq i} \gamma_{ij} (\mu_i - \mu_j). \quad (4)$$

Here the potentials μ_i are intended to be position dependent along the equilibration path between injector and detector. The terms $\gamma_{ij} = \gamma_{ji}$ model a uniform coupling between channels i and j [see Fig. 3(b)]. These parameters encapsulate any equilibration process in our model, giving us a quantity related to the average equilibration lengths $\ell_{ij}^{\text{eq}} = \gamma_{ij}^{-1}$ between channels i and j . We can numerically calculate the whole set of γ_{ij} by performing an equal amount of independent measurements at the detector, each time setting the barrier filling factors to integer values such that $\nu_I \leq \nu_D$ and $\nu_I, \nu_D < \nu_B$ [42].

Starting with $\nu_B = 8$ in Fig. 3(c), we observe that spin-conserving coupling terms dominate, while spin-flip terms can be more than 1 order of magnitude smaller. Spin-selective tunneling couples not only the spatially closest channels with parallel spin (channels 1 and 3), but also terms like γ_{15} and γ_{26} are much larger than spin-flip terms coupling nearest neighbors. This shows that it is more likely for electrons to tunnel a larger distance without flipping their spin rather than tunneling through a thinner barrier undergoing a spin-flip event.

Increasing the field and decreasing ν_B at constant density progressively decouples the channels. In Figs. 3(d) and 3(e)

we observe a reduction of the long-distance coupling terms γ_{15} and γ_{26} . The spin-selective coupling terms γ_{13} and γ_{24} appear to increase with the magnetic field, but the extraction of a precise value is difficult in the extreme cases and due to mesoscopic fluctuations [42]. In Fig. 3(f) the trend continues and also short-range spin-selective coefficients decrease. Finally, for $\nu_B \leq 4$, all the integer channels are mostly decoupled, either too far removed towards the bulk or limited by the frequency of spin-flip events.

In this Letter, we analyzed our data based on the well-established edge channel picture of the integer quantum Hall effect, finding that channels with parallel spin selectively couple with each other, while flipping the spin of electrons is much less likely. At low enough fields, spin-conserving tunneling even couples modes separated by several compressible and incompressible stripes instead of only neighboring channels with parallel spin. In general, the equilibration process is influenced by experimental parameters, like magnetic field and temperature [49], and by sample properties, such as material quality and heterostructure design. Controlling the transfer of particles between channels could lead to the use of edge modes as spin rails to transport well-defined magnetic moments in quantum computation experiments [50–52]. The presence of spin-selective signatures at low field would help to integrate such a technology with others that do not tolerate or require high fields.

In the fractional regime, a precise knowledge of the equilibration length is sought after to improve experiments involving interferometers and other confined systems [53,54], anyonic statistics [55,56], the thermal conductance of exotic states [57–59] and the complex edge reconstruction associated with fractional states like $2/3$ [60,61] and $5/2$ [62,63]. Investigating the fractional quantum Hall regime is a natural next step and we believe that the techniques established in this Letter could complement investigations of edge reconstruction and the formation of stripes with fractional filling factor in a variety of materials [27].

We thank M. Shayegan for illuminating discussions. We acknowledge support from the ETH FIRST laboratory and financial support from the National Center of Competence in Research “QSIT—Quantum Science and Technology.”

* gnicoli@phys.ethz.ch

- [1] M. Z. Hasan and C. L. Kane, Colloquium: Topological insulators, *Rev. Mod. Phys.* **82**, 3045 (2010).
- [2] K. v. Klitzing, G. Dorda, and M. Pepper, New Method for High-Accuracy Determination of the Fine-Structure Constant Based on Quantized Hall Resistance, *Phys. Rev. Lett.* **45**, 494 (1980).
- [3] D. C. Tsui, H. L. Stormer, and A. C. Gossard, Two-Dimensional Magnetotransport in the Extreme Quantum Limit, *Phys. Rev. Lett.* **48**, 1559 (1982).

- [4] B. I. Halperin, Quantized Hall conductance, current-carrying edge states, and the existence of extended states in a two-dimensional disordered potential, *Phys. Rev. B* **25**, 2185 (1982).
- [5] R. Prange and S. M. Girvin, *The Quantum Hall Effect* (Springer, New York, 1990).
- [6] R. J. Haug, Edge-state transport and its experimental consequences in high magnetic fields, *Semicond. Sci. Technol.* **8**, 131 (1993).
- [7] S. W. Hwang, D. C. Tsui, and M. Shayegan, Experimental evidence for finite-width edge channels in integer and fractional quantum Hall effects, *Phys. Rev. B* **48**, 8161 (1993).
- [8] B. W. Alphenaar, P. L. McEuen, R. G. Wheeler, and R. N. Sacks, Selective equilibration among the current-carrying states in the quantum Hall regime, *Phys. Rev. Lett.* **64**, 677 (1990).
- [9] R. J. Haug, J. Kucera, P. Streda, and K. von Klitzing, Scattering experiments in two-dimensional systems in the presence of quantizing magnetic fields, *Phys. Rev. B* **39**, 10892 (1989).
- [10] S. Komiyama, H. Hirai, M. Ohsawa, Y. Matsuda, S. Sasa, and T. Fujii, Inter-edge-state scattering and nonlinear effects in a two-dimensional electron gas at high magnetic fields, *Phys. Rev. B* **45**, 11085 (1992).
- [11] G. Müller, D. Weiss, A. V. Khaetskii, K. von Klitzing, S. Koch, H. Nickel, W. Schlapp, and R. Lösch, Equilibration length of electrons in spin-polarized edge channels, *Phys. Rev. B* **45**, 3932 (1992).
- [12] Y. Takagaki, K. J. Friedland, J. Herfort, H. Kostial, and K. Ploog, Inter-edge-state scattering in the spin-polarized quantum Hall regime with current injection into inner states, *Phys. Rev. B* **50**, 4456 (1994).
- [13] S. Washburn, A. B. Fowler, H. Schmid, and D. Kern, Quantized Hall Effect in the Presence of Backscattering, *Phys. Rev. Lett.* **61**, 2801 (1988).
- [14] Y. Acremann, T. Heinzel, K. Ensslin, E. Gini, H. Melchior, and M. Holland, Individual scatterers as microscopic origin of equilibration between spin-polarized edge channels in the quantum Hall regime, *Phys. Rev. B* **59**, 2116 (1999).
- [15] R. J. Haug, A. H. MacDonald, P. Streda, and K. von Klitzing, Quantized Multichannel Magnetotransport through a Barrier in Two Dimensions, *Phys. Rev. Lett.* **61**, 2797 (1988).
- [16] G. Müller, E. Diessel, D. Weiss, K. von Klitzing, K. Ploog, H. Nickel, W. Schlapp, and R. Lösch, Influence of interedge channel scattering on the magneto-transport of 2D-systems, *Surf. Sci.* **263**, 280 (1992).
- [17] E. V. Deviatov and A. Lorke, Separately contacted edge states at high imbalance in the integer and fractional quantum Hall effect regime, *Phys. Status Solidi (b)* **245**, 366 (2008).
- [18] A. Grivnin, H. Inoue, Y. Ronen, Y. Baum, M. Heiblum, V. Umansky, and D. Mahalu, Nonequilibrated Counterpropagating Edge Modes in the Fractional Quantum Hall Regime, *Phys. Rev. Lett.* **113**, 266803 (2014).
- [19] C. Lin, R. Eguchi, M. Hashisaka, T. Akiho, K. Muraki, and T. Fujisawa, Charge equilibration in integer and fractional quantum Hall edge channels in a generalized Hall-bar device, *Phys. Rev. B* **99**, 195304 (2019).

- [20] T. Maiti, P. Agarwal, S. Purkait, G. J. Sreejith, S. Das, G. Biasiol, L. Sorba, and B. Karmakar, Magnetic-Field-Dependent Equilibration of Fractional Quantum Hall Edge Modes, *Phys. Rev. Lett.* **125**, 076802 (2020).
- [21] Y. Y. Wei, J. Weis, K. v. Klitzing, and K. Eberl, Edge Strips in the Quantum Hall Regime Imaged by a Single-Electron Transistor, *Phys. Rev. Lett.* **81**, 1674 (1998).
- [22] P. Weitz, E. Ahlswede, J. Weis, K. v. Klitzing, and K. Eberl, A low-temperature scanning force microscope for investigating buried two-dimensional electron systems under quantum Hall conditions, *Appl. Surf. Sci.* **157**, 349 (2000).
- [23] J. Huels, J. Weis, J. Smet, K. v. Klitzing, and Z. R. Wasilewski, Long time relaxation phenomena of a two-dimensional electron system within integer quantum Hall plateau regimes after magnetic field sweeps, *Phys. Rev. B* **69**, 085319 (2004).
- [24] T. Klaffs, V. A. Krupenin, J. Weis, and F. J. Ahlers, Eddy currents in the integer quantum Hall regime spatially resolved by multiple single-electron transistor electrometers, *Physica E* **22**, 737 (2004).
- [25] L. P. Kouwenhoven, B. J. van Wees, N. C. van der Vaart, C. J. P. M. Harmans, C. E. Timmering, and C. T. Foxon, Selective Population and Detection of Edge Channels in the Fractional Quantum Hall Regime, *Phys. Rev. Lett.* **64**, 685 (1990).
- [26] A. M. Chang and J. E. Cunningham, Transport Evidence for Phase Separation into Spatial Regions of Different Fractional Quantum Hall Fluids Near the Boundary of a Two-Dimensional Electron Gas, *Phys. Rev. Lett.* **69**, 2114 (1992).
- [27] R. Sabo, I. Gurman, A. Rosenblatt, F. Lafont, D. Banitt, J. Park, M. Heiblum, Y. Gefen, V. Umansky, and D. Mahalu, Edge reconstruction in fractional quantum Hall states, *Nat. Phys.* **13**, 491 (2017).
- [28] F. Amet, J. R. Williams, K. Watanabe, T. Taniguchi, and D. Goldhaber-Gordon, Selective Equilibration of Spin-Polarized Quantum Hall Edge States in Graphene, *Phys. Rev. Lett.* **112**, 196601 (2014).
- [29] D. S. Wei, T. van der Sar, J. D. Sanchez-Yamagishi, K. Watanabe, T. Taniguchi, P. Jarillo-Herrero, B. I. Halperin, and A. Yacoby, Mach-Zehnder interferometry using spin- and valley-polarized quantum Hall edge states in graphene, *Sci. Adv.* **3**, e1700600 (2017).
- [30] K. Zimmermann, A. Jordan, F. Gay, K. Watanabe, T. Taniguchi, Z. Han, V. Bouchiat, H. Sellier, and B. Saccépé, Tunable transmission of quantum Hall edge channels with full degeneracy lifting in split-gated graphene devices, *Nat. Commun.* **8**, 14983 (2017).
- [31] C. Kumar, S. K. Srivastav, and A. Das, Equilibration of quantum Hall edges in symmetry-broken bilayer graphene, *Phys. Rev. B* **98**, 155421 (2018).
- [32] G. Müller, D. Weiss, S. Koch, K. von Klitzing, H. Nickel, W. Schlapp, and R. Lösch, Edge channels and the role of contacts in the quantum Hall regime, *Phys. Rev. B* **42**, 7633 (1990).
- [33] J. Faist, P. Guéret, and H. P. Meier, Interior contacts for probing the equilibrium between magnetic edge channels in the quantum Hall effect, *Phys. Rev. B* **43**, 9332 (1991).
- [34] M. T. Woodside, C. Vale, P. L. McEuen, C. Kadow, K. D. Maranowski, and A. C. Gossard, Imaging interedge-state scattering centers in the quantum Hall regime, *Phys. Rev. B* **64**, 041310(R) (2001).
- [35] M. Berl, L. Tiemann, W. Dietsche, H. Karl, and W. Wegscheider, Structured back gates for high-mobility two-dimensional electron systems using oxygen ion implantation, *Appl. Phys. Lett.* **108**, 132102 (2016).
- [36] J. Scharnetzky, J. M. Meyer, M. Berl, C. Reichl, L. Tiemann, W. Dietsche, and W. Wegscheider, A novel planar back-gate design to control the carrier concentrations in GaAs-based double quantum wells, *Semicond. Sci. Technol.* **35**, 085019 (2020).
- [37] G. Nicolí, P. Märki, B. A. Bräm, M. P. Rösli, S. Hannel, A. Hofmann, C. Reichl, W. Wegscheider, T. Ihn, and K. Ensslin, Quantum dot thermometry at ultra-low temperature in a dilution refrigerator with a 4He immersion cell, *Rev. Sci. Instrum.* **90**, 113901 (2019).
- [38] Even though our setup in general could reach a lower base temperature, during this cool down the setup suffered from a higher thermal load, likely due to a problem with the magnet switch heater. We decided to continue the investigation nevertheless as a lower temperature was not critical for this experiment.
- [39] To be precise, in order to render the bulk density as uniform as possible, we energize the top gates with a small positive bias of $\approx 30\text{--}50$ mV. This counteracts the density modulation due to the presence alone of the gates on the surface of the device.
- [40] M. Büttiker, Four-Terminal Phase-Coherent Conductance, *Phys. Rev. Lett.* **57**, 1761 (1986).
- [41] S. Datta, *Electronic Transport in Mesoscopic Systems*, Cambridge Studies in Semiconductor Physics and Microelectronic Engineering (Cambridge University Press, Cambridge, England, 1995).
- [42] See Supplemental Material at <http://link.aps.org/supplemental/10.1103/PhysRevLett.128.056802> for details about sample fabrication and tuning, for a discussion of the propagator model and for additional data measured with different lengths and different side gate voltages.
- [43] Channels with $\tilde{\mu}_i^0 = 0$ end up sometimes having potential higher than channel 1. Impurities may modulate the equilibration along the way such that channel 1 can first strongly equilibrate with another one with parallel spin and then partially decouple from it to scatter electrons with a spin flip into a neighboring channel, resulting in channel 1 having lower electrochemical potential at the detector than some other channel with parallel spin.
- [44] D. B. Chklovskii, B. I. Shklovskii, and L. I. Glazman, Electrostatics of edge channels, *Phys. Rev. B* **46**, 4026 (1992).
- [45] R. R. Gerhardts, The effect of screening on current distribution and conductance quantisation in narrow quantum Hall systems, *Phys. Status Solidi (b)* **245**, 378 (2008).
- [46] K. Lier and R. R. Gerhardts, Self-consistent calculations of edge channels in laterally confined two-dimensional electron systems, *Phys. Rev. B* **50**, 7757 (1994).
- [47] D. L. Kovrizhin and J. T. Chalker, Equilibration of integer quantum Hall edge states, *Phys. Rev. B* **84**, 085105 (2011).
- [48] G. Müller, D. Weiss, K. von Klitzing, K. Ploog, H. Nickel, W. Schlapp, and R. Lösch, Confinement-potential tuning: From nonlocal to local transport, *Phys. Rev. B* **46**, 4336 (1992).

- [49] H. Hirai, S. Komiyama, S. Fukatsu, T. Osada, Y. Shiraki, and H. Toyoshima, Dependence of inter-edge-channel scattering on temperature and magnetic field: Insight into the edge-confining potential, *Phys. Rev. B* **52**, 11159 (1995).
- [50] P. Roulleau, F. Portier, D. C. Glatli, P. Roche, A. Cavanna, G. Faini, U. Gennser, and D. Mailly, Direct Measurement of the Coherence Length of Edge States in the Integer Quantum Hall Regime, *Phys. Rev. Lett.* **100**, 126802 (2008).
- [51] H. Duprez, E. Sivre, A. Anthore, A. Aassime, A. Cavanna, A. Ouerghi, U. Gennser, and F. Pierre, Macroscopic Electron Quantum Coherence in a Solid-State Circuit, *Phys. Rev. X* **9**, 021030 (2019).
- [52] A. Rosenblatt, S. Konyzheva, F. Lafont, N. Schiller, J. Park, K. Snizhko, M. Heiblum, Y. Oreg, and V. Umansky, Energy Relaxation in Edge Modes in the Quantum Hall Effect, *Phys. Rev. Lett.* **125**, 256803 (2020).
- [53] M. P. Rössli, L. Brem, B. Kratochwil, G. Nicolí, B. A. Braem, S. Hennel, P. Märki, M. Berl, C. Reichl, W. Wegscheider, K. Ensslin, T. Ihn, and B. Rosenow, Observation of quantum Hall interferometer phase jumps due to a change in the number of bulk quasiparticles, *Phys. Rev. B* **101**, 125302 (2020).
- [54] M. P. Rössli, M. Hug, G. Nicolí, P. Märki, C. Reichl, B. Rosenow, W. Wegscheider, K. Ensslin, and T. Ihn, Fractional Coulomb blockade for quasiparticle tunneling between edge channels, *Sci. Adv.* **7**, eabf5547 (2021).
- [55] J. Nakamura, S. Fallahi, H. Sahasrabudhe, R. Rahman, S. Liang, G. C. Gardner, and M. J. Manfra, Aharonov–Bohm interference of fractional quantum Hall edge modes, *Nat. Phys.* **15**, 563 (2019).
- [56] H. Bartolomei, M. Kumar, R. Bisognin, A. Marguerite, J.-M. Berroir, E. Bocquillon, B. Plaçais, A. Cavanna, Q. Dong, U. Gennser, Y. Jin, and G. Fève, Fractional statistics in anyon collisions, *Science* **368**, 173 (2020).
- [57] G. Granger, J. P. Eisenstein, and J. L. Reno, Observation of Chiral Heat Transport in the Quantum Hall Regime, *Phys. Rev. Lett.* **102**, 086803 (2009).
- [58] V. Venkatachalam, S. Hart, L. Pfeiffer, K. West, and A. Yacoby, Local thermometry of neutral modes on the quantum Hall edge, *Nat. Phys.* **8**, 676 (2012).
- [59] M. Banerjee, M. Heiblum, A. Rosenblatt, Y. Oreg, D. E. Feldman, A. Stern, and V. Umansky, Observed quantization of anyonic heat flow, *Nature (London)* **545**, 75 (2017).
- [60] F. Lafont, A. Rosenblatt, M. Heiblum, and V. Umansky, Counter-propagating charge transport in the quantum Hall effect regime, *Science* **363**, 54 (2019).
- [61] Y. Cohen, Y. Ronen, W. Yang, D. Banitt, J. Park, M. Heiblum, A. D. Mirlin, Y. Gefen, and V. Umansky, Synthesizing a $\nu = 2/3$ fractional quantum Hall effect edge state from counter-propagating $\nu = 1$ and $\nu = 1/3$ states, *Nat. Commun.* **10**, 1920 (2019).
- [62] M. Banerjee, M. Heiblum, V. Umansky, D. E. Feldman, Y. Oreg, and A. Stern, Observation of half-integer thermal Hall conductance, *Nature (London)* **559**, 205 (2018).
- [63] B. Dutta, W. Yang, R. A. Melcer, H. K. Kundu, M. Heiblum, V. Umansky, Y. Oreg, A. Stern, and D. Mross, Novel method distinguishing between competing topological orders, *arXiv:2101.01419*.